ecologies

MDPI

Article

Spectral Patterns of Pixels and Objects of the Forest Phytophysiognomies in the Anauá National Forest, Roraima State, Brazil

Tiago Monteiro Condé [1,*], Niro Higuchi [2], Adriano José Nogueira Lima [2], Moacir Alberto Assis Campos [2], Jackelin Dias Condé [1], André Camargo de Oliveira [1] and Dirceu Lucio Carneiro de Miranda [3]

[1] Forest Management and Geotecnology Laboratory (LMFG), State University of Roraima (UERR), Av. Senador Helio Campos, Rorainópolis 69373-000, RR, Brazil; jackelin.dias20@gmail.com (J.D.C.); acco9995@yahoo.com.br (A.C.d.O.)

[2] Forest Management Laboratory (LMF), National Institute of Amazonian Research (INPA), Av. André Araújo, Manaus 69060-001, AM, Brazil; niro@inpa.gov.br (N.H.); adrianolmf@gmail.com (A.J.N.L.); camposmoacir@gmail.com (M.A.A.C.)

[3] Forest Management Laboratory (LMF), Federal University of Mato Grosso (UFMT), Av. Alexandre Ferronato, Sinop 78550-728, MT, Brazil; mirandaufpr@yahoo.com.br

* Correspondence: tiagonafloresta@gmail.com

Abstract: Forest phytophysiognomies have specific spatial patterns that can be mapped or translated into spectral patterns of vegetation. Regions of spectral similarity can be classified by reference to color, tonality or intensity of brightness, reflectance, texture, size, shape, neighborhood influence, etc. We evaluated the power of accuracy of supervised classification algorithms via per-pixel (maximum likelihood) and geographic object-based image analysis (GEOBIA) for distinguishing spectral patterns of the vegetation in the northern Brazilian Amazon. A total of 280 training samples (70%) and 120 validation samples (30%) of each of the 11 vegetation cover and land-use classes (N = 4400) were classified based on differences in their visible (RGB), near-infrared (NIR), and medium infrared (SWIR 1 or MIR) Landsat 8 (OLI) bands. Classification by pixels achieved a greater accuracy (Kappa = 0.75%) than GEOBIA (Kappa = 0.72%). GEOBIA, however, offers a greater plasticity and the possibility of calibrating the spectral rules associated with vegetation indices and spatial parameters. We conclude that both methods enabled precision spectral separations (0.45–1.65 μm), contributing to the distinctions between forest phytophysiognomies and land uses—strategic factors in the planning and management of natural resources in protected areas in the Amazon region.

Keywords: Amazon; GEOBIA; image classification; image segmentation; Landsat 8

check for updates

Citation: Condé, T.M.; Higuchi, N.; Lima, A.J.N.; Campos, M.A.A.; Condé, J.D.; de Oliveira, A.C.; de Miranda, D.L.C. Spectral Patterns of Pixels and Objects of the Forest Phytophysiognomies in the Anauá National Forest, Roraima State, Brazil. *Ecologies* **2023**, *4*, 686–703. https://doi.org/10.3390/ecologies4040045

Academic Editor: José Ramón Arévalo Sierra

Received: 31 August 2023
Revised: 16 October 2023
Accepted: 18 October 2023
Published: 28 October 2023

1. Introduction

Digital image processing (DIP) faces a new paradigm in which conventional classification by pixels, considered the smallest, central, and exclusive carrier element of geographic information [1,2], is refined via either an object-based image analysis (OBIA) approach [3–8] or geographic object-based image analysis (GEOBIA) [9–11]. New paradigms require new methodological conceptions, considering that researchers [12,13] have already reported problems with conventional approaches at the pixel level related to multiple scaling processes, mixed pixels, spatial information degradation, and unstable effects in environmental modeling, such as the "salt-and-pepper" effect [14]. With technological advances and the availability of medium to high spatial resolution data, the degrees of detail and the quantities of information generated have greatly increased, and there is a need to adjust the regionalization of information by DIP, highlighting segmentation technique processes in hierarchizations as vital to the classification and understanding of the dynamics of vegetation cover and land-use changes [11,14].

Environmental studies related to the detection of vegetation cover and land-use changes in the Amazon region require the continuous evolution of DIP techniques in remote-sensing software and geographic information systems, as well as computers with greater processing capacities that could allow the rapid detection of deforestation and forest degradation [15–18], and therefore facilitate environmental monitoring, inspections, and the conservation and protection of the environmental services provided by Brazilian Amazonian forests [19,20]. The GEOBIA approach considers the delimitation of homogeneous geographic objects as the basis for the later processing of the hierarchization of upper and lower levels via different processing algorithms, and determining whether they can be inherited or not [7,9,10]. In practice, satellite images are segmented as "pieces of a puzzle" into geographic objects with similar characteristics of brightness, reflectance, color, texture, area, shape, and neighborhood influences, etc., which are elaborated by a set of rules that allow associations between the objects, vegetation indices, and spatial parameters in the landscape, at different spatial scales, and in different hierarchies. Conventional pixel procedures are purely statistical and based on differences in the behaviors of objects and their spatial and spectral relationships [12,13]. In a per-pixel approach, supervised classification makes use of samples of regions of interest (ROI) used for training and validation, which are usually performed via algorithms such as maximum likelihood, support vector machine, etc., and obtain good results from a statistical point of view. Mixed pixels, however, are considered sources of errors and are corrected by spectral unmixing [21–23].

The spectral behavior of an object can be defined using its reflectance values along the electromagnetic spectrum—also called its spectral signature or spectral pattern [24,25]. Objects on the Earth's surface reflect, absorb, and transmit electromagnetic radiation in ratios that vary according to their biophysical–chemical characteristics [24–26], making it possible to distinguish different regions of interest (ROI) by their spectral characteristic in the landscape via remote sensing and DIP. The difference in the present spectral pattern approach was that we compared different supervised classification methods of natural ecosystems in the Brazilian Amazon under constant human pressure to expand land use. The principal questions addressed in this study were: (i) Can the spectral patterns of vegetation obtained from different color combinations of visible (RGB) and infrared (NIR and SWIR 1 or MIR) bands of Landsat 8 images allow us to distinguish between forest phytophysiognomies in the northern Brazilian Amazon? (ii) Can we measure the spectral separability of vegetation cover classes? (iii) Which supervised classification method (pixel-based—maximum likelihood; or geographic object-based image analysis—GEOBIA) provides greater accuracy in this context?

2. Materials and Methods

2.1. Study Area and Data Collection

The study area (102,750 km^2) is covered by a mosaic of reflectance images (path 232; rows 059–060) of the Landsat 8 [OLI: Operational Land Imager], obtained from the USGS website (http://earthexplorer.usgs.gov/). The daytime summer season images (04 October 2015 and 10 January 2017) have an incidence of cloud cover of less than 10%. The Anauá National Forest is a protected area in the extreme northern Brazilian Amazon, in Roraima State. It is a federal conservation area managed by the Chico Mendes Institute of Biodiversity (ICMBio) and covers approximately 2600 km^2 (Figure 1). It is part of the white-sand ecosystems of the Brazilian Amazon, a region with a high degree of endemism, although few botanical surveys have been conducted there [27–30]. It is marked by seasonal hydrological influences [31], with different degrees of hydro-morphism [32], and is exposed to increasing atmospheric carbon emissions caused by human actions associated with deforestation for cattle ranching [33–35], forest degradation, illegal selective logging, and forest fires [16–18,20]. The Anauá National Forest was created in 2005, although its management plan was only approved in 2022 [36].

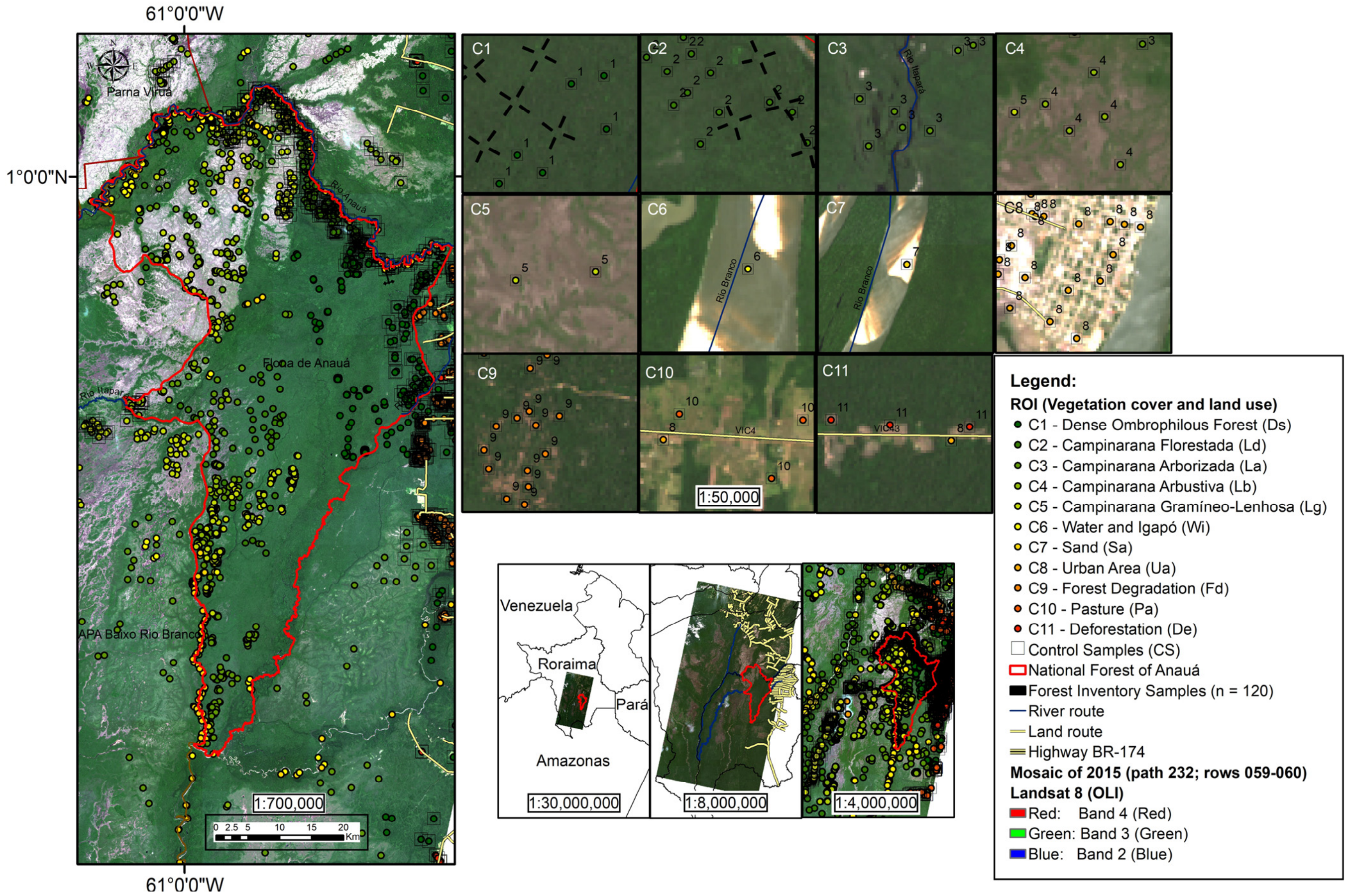

Figure 1. The study area (102,750 km^2) is centered on the Anauá National Forest in Roraima State, Brazil, covered by a mosaic of Landsat 8 (OLI) reflectance images (path 232, rows 059–060).

To more accurately represent reality in the field, we classified 2500 control samples (CS) using a handheld GPS (Garmin Etrex, UTM Projection, Datum WGS84), recording their spatial coordinates, and making photographic records of the in situ landscape, into 11 vegetation cover and land-use classes (C), following the classification system of the Brazilian Institute of Geography and Statistics—IBGE [37] (Table 1). The CS were obtained through joint operations of research, inspection, and environmental monitoring, with the participation of ICMBio, the State Foundation for the Environment and Water Resources (FEMARH), the Independent Company of Environmental Policing of the Military Police (CIPA), the State University of Roraima (UERR), and the Laboratory of Forest Management of the National Institute of Amazonian Research (LMF/INPA). Approximately 1266 km were navigated along the Branco, Anauá, Itapará, and Jaburu rivers, as well as several streams, during the inventory of the Anauá National Forest, and in support of the National Action Plan for the Conservation of the Amazonian Manatee (*Trichechus inunguis*) coordinated by the Roraima ICMBio [38]. During the installation of 120 plots (0.25 ha each; 30 ha total) for a forest inventory (IF) of trees with diameters at breast height (DBH) $\geq$ 10 cm, 74 km were covered by walking within the Anauá National Forest [18]. Additionally, 3000 km were covered along roads surrounding the Anauá National Forest and neighboring areas in the municipalities of Cantá, Caracaraí, Mucajaí, Iracema, and Rorainópolis, to detect changes in vegetation cover and land use during the period between 2013 and 2017.

Table 1. Classes of vegetation cover and land use in the Anauá National Forest, Roraima State, Brazil.

Class	Vegetation Cover and Land Use	Initials	Description	Colors ROI
C1	Dense Ombrophilous Forest	Ds	Dense forest cover, high textural roughness, no soil exposure.	
C2	Campinarana Florestada	Ld	Dense forest cover, medium textural roughness, no soil exposure.	
C3	Campinarana Arborizada	La	Environment with trees and shrubs, with slight soil exposure.	
C4	Campinarana Arbustiva	Lb	Environment with shrubs and average soil exposure.	
C5	Campinarana Gramíneo-Lenhosa	Lg	Environment with grasses and high soil exposure.	
C6	Water and Igapó	Wi	Rivers, streams, and flooded environments	
C7	Sand	Sa	Environment with sandy soils.	
C8	Urban area	Ua	Anthropically altered areas with different degrees of urbanization.	
C9	Forest Degradation	Fd	Areas impacted by illegal selective logging.	
C10	Pasture	Pa	Pasture areas in different states of conservation.	
C11	Deforestation	De	Areas with forest cover removed, with soil exposure.	

Forest physiognomies (Ds, Ld, La, Lb, Lg) were classified according to the Brazilian Institute of Geography and Statistics—IBGE [37]; ROI colors were assigned to differentiate regions of interest during training and validation.

2.2. Data Analysis and Digital Image Processing

Initially, digital image processing (DIP) was performed to convert digital numbers (DN) to top of atmosphere reflectance (TOA) physical units, maintaining the 16-bit radiometric resolution, as described in the Landsat 8 (L8) Data Users Handbook—Version 5.0 (2019). Subsequently, exploratory DIP analyses of the control samples (CS) and the reflectance images were performed. To detect the spectral patterns of the forest phytophysiognomies in Anauá National Forest, 2500 CS were used as field references for the later stage of DIP, with the selection of 4400 ROI samples of vegetation cover and land use exhibiting spectral homogeneity and similar statistical parameters in relation to the reflectance of the five bands analyzed (0.45–1.65 µm) [39]. The ROI were divided into 280 training samples (70%) and 120 validation samples (30%) in each class mapped, composing 4400 mosaic ROI samples (102,750 Km^2). We evaluated the statistics (mean, median, range, standard deviation, variance, correlation matrix, and confidence interval—$CI_{95\%}$) of the ROI reflectance values, analysis of variance (ANOVA), and pairwise comparison test (Tukey) in R programming language using R Studio software—Version 2022.12.0 [40] via the corrplot R package. In this way, three (3) color compositions were evaluated in visible (RGB) and infrared (NIR and SWIR 1) bands, with contrast enhancement in the stretch image histogram with standard deviations (n = 2.5) (Figure 2).

2.3. The Spectral Behavior of the Vegetation Indices and Fractional Coverage Image Index

We used two vegetation indices (NDVI and NDWI) [22,41,42], based on spectral reflectance behavior, to indirectly describe the remote sensing of photosynthesis and the presence of water in the internal structures of the plants. We used a fractional cover image (FCI) index [16,17], derived from automatic processing by CLASlite Forest Monitoring Technology Software—Version 3.2. The FCI represents the pixel subdivided into 3 fractions: PV (the fractional cover of photosynthetic vegetation, 0–100%); NPV (the fractional cover of non-photosynthetic vegetation, 0–100%); and BARE (the fractional cover of bare substrate, 0–100%).

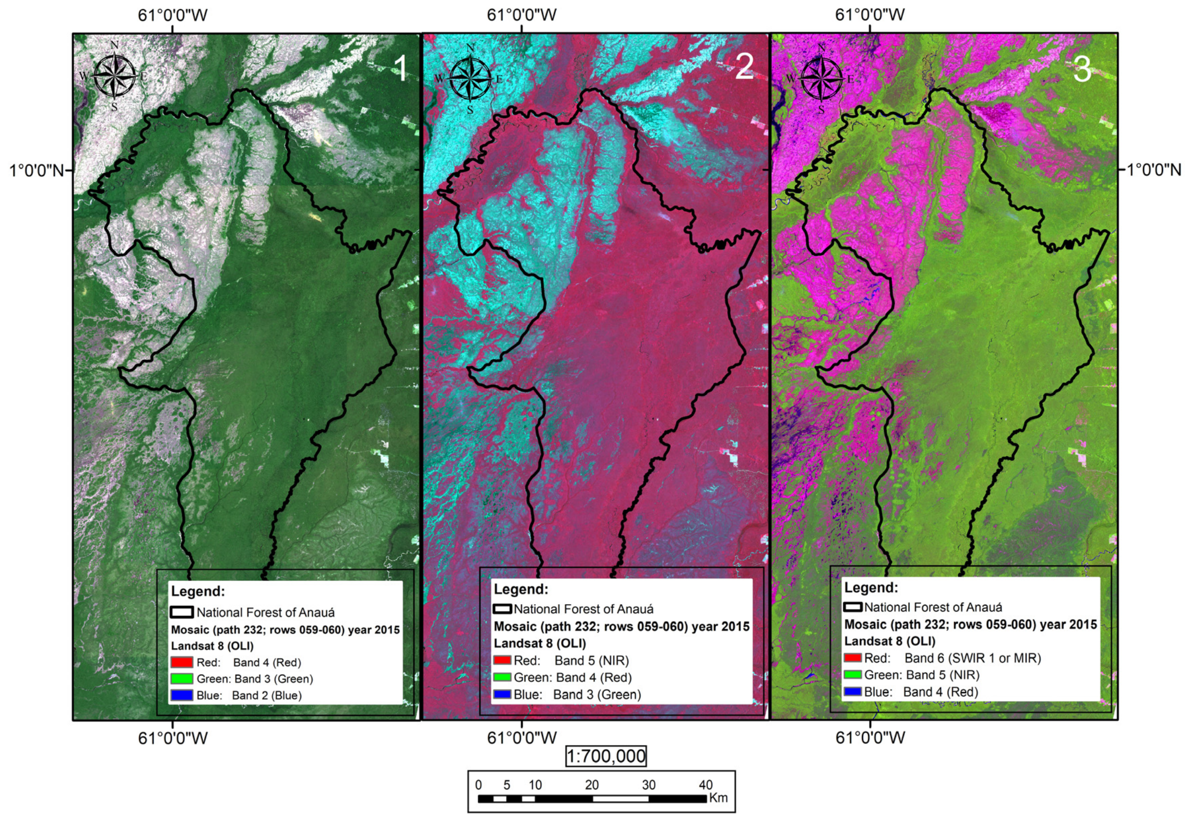

Figure 2. Color compositions of reflectance in visible (RGB), near-infrared (NIR), and medium infrared (SWIR 1 or MIR) wavelengths of Landsat 8 (OLI) images of the Anauá National Forest, where: (**1**) Visible {R(4)G(3)B(2)}: R [Red b4] = 0.64–0.67 µm; G [Green b3] = 0.53–0.59 µm; B [Blue b2] = 0.45–0.51 µm; (**2**) Near infrared {R(5)G(4)B(3)}: R [NIR b5] = 0.85–0.88 µm; G [Red b4] = 0.45–0.51 µm; B [Green b3] = 0.53–0.59 µm; (**3**) Mean infrared {R(6)G(5)B(4)}: R [SWIR 1 or MIR b6] = 1.57–1.65 µm; G [NIR b5] = 0.85–0.88 µm; R [Red b4] = 0.45–0.51 µm.

2.4. Pixel-Based Supervised Classification

Supervised classification of digital images per pixel was performed via the maximum likelihood algorithm using ENVI—Version 5.1 [CLASSIC] software, which assumes that the statistics of each class in each band are normally distributed and calculates the probability of a particular pixel belonging to a specific class [2,22]. This classification process was performed in two stages: (1) Training, with training samples (70%); and (2) Validation, with validation samples (30%), both considering ROI samples of the 11 vegetation cover and land-use classes. We used a 10,000 scale factor to divide TOA reflectance values (Landsat 8) and to graphically represent the spectral patterns on a scale from 0 to 1%. Accuracy was also evaluated via a confusion matrix (or error matrix) in relation to the 3-color composition, quantifying the overall score and Kappa index [22,43] (Supplementary Material: Figures S1–S4). We performed several simulations before choosing the final five bands (0.45–1.65 µm). We tested the inclusion of the seven bands (b1 to b7) with different combinations but obtained only a low precision (overall < 60%; Kappa < 0.56).

2.5. Supervised Classification of Geographic Object-Based Image Analysis (GEOBIA)

GEOBIA [9–11] was performed in 5 steps via Trimble eCognition Developer 9 software (Figure 3). A set of rules defined in a hierarchical process tree was used, gathering information about the textural characteristics of the images, as described by Haralick [44], spatial statistics (mean and standard deviation) of the variation in reflectance values of the visible (RGB) and infrared (NIR and MIR) bands, vegetation index thresholds (NDVI and

NDWI), and the edge effects of pixels in the neighborhood. Those rules were defined to increase accuracy while separating the spectral patterns of the different classes.

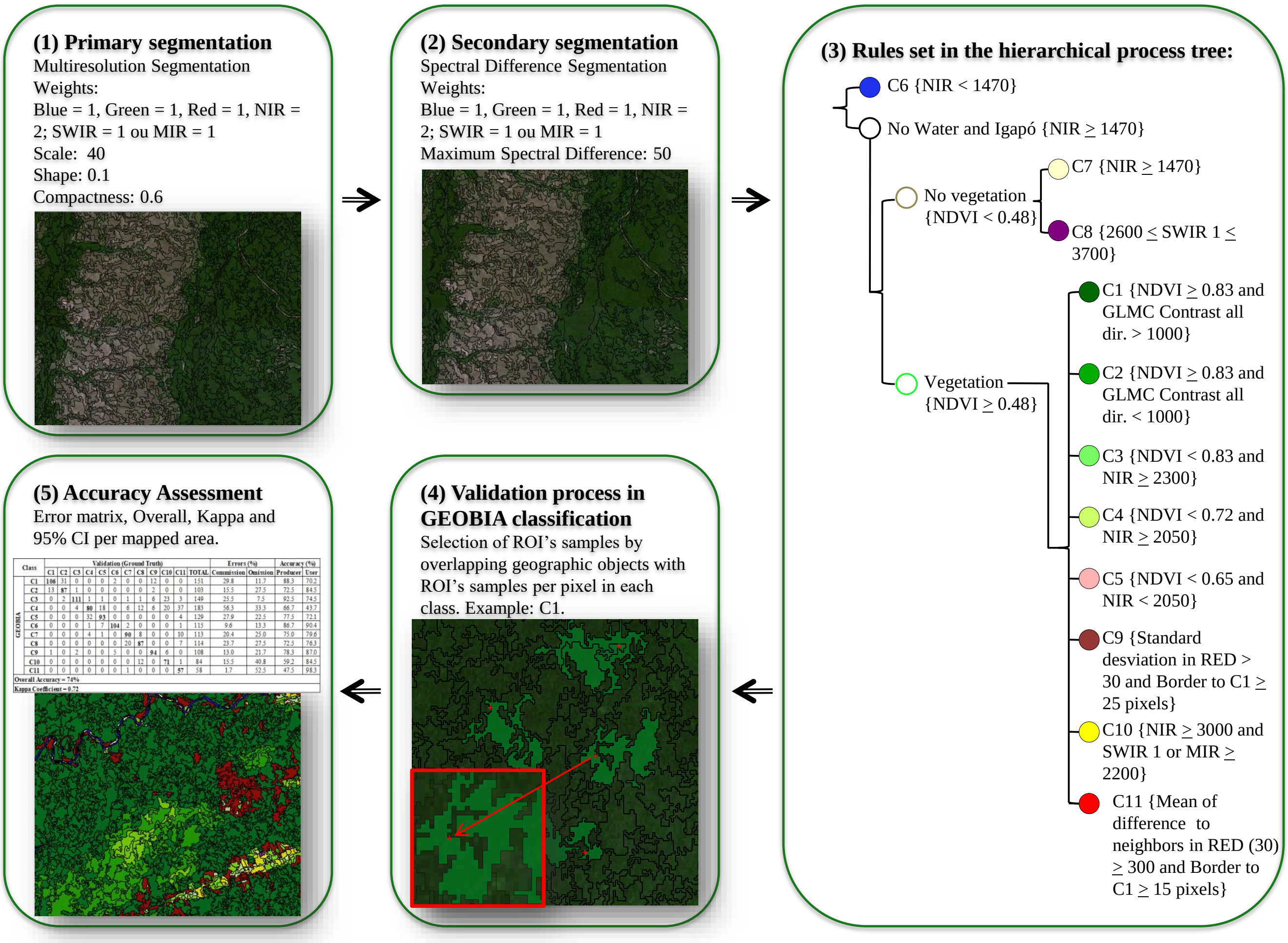

Figure 3. Supervised classification of Geographic Object-Based Image Analysis (GEOBIA) in 5 steps. Using reflectance values without a conversion factor (10,000).

3. Results

3.1. Vegetation Spectral Patterns

The spectral patterns of the 11 vegetation cover and land-use classes related to visible and infrared reflectance (NIR and SWIR 1 or MIR) were generated from 4400 ROI samples per pixel of the landscape mosaic (102,750 km^2) covering the Anauá National Forest, in Roraima State, Brazil (Table 2).

Table 2. Spectral patterns of 11 vegetation cover and land-use classes from ROI samples per pixel (N = 4400) in terms of their visible (RGB) and infrared (NIR and SWIR 1 or MIR) bands.

Class	Vegetation Cover and Land Use	Spectral Patterns
C1	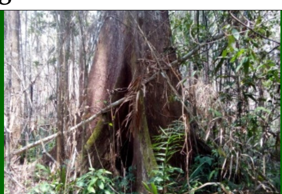 Dense Ombrophilous Forest (Ds)	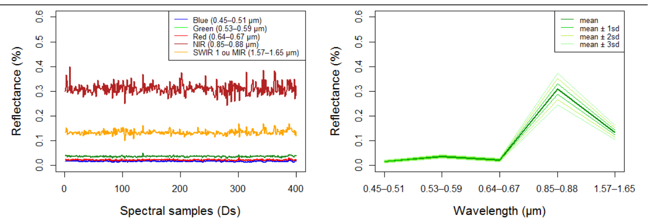

Table 2. *Cont.*

Class	Vegetation Cover and Land Use	Spectral Patterns
C2	 Campinarana Florestada (Ld)	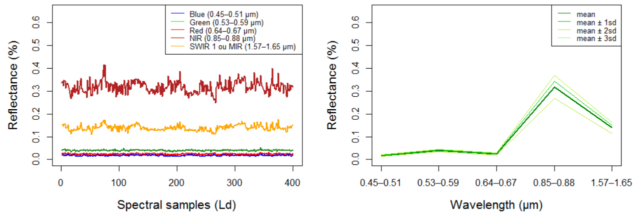
C3	 Campinarana Arborizada (La)	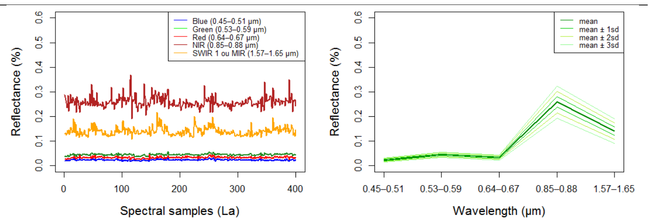
C4	 Campinarana Arbustiva (Lb)	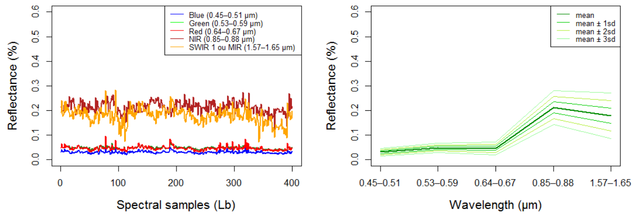
C5	 Campinarana Gramíneo-Lenhosa (Lg)	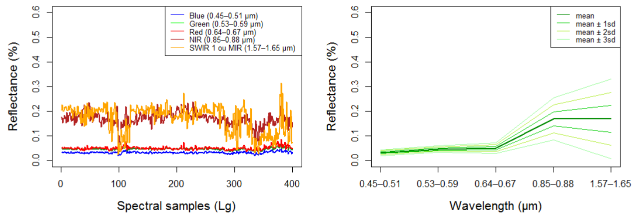
C6	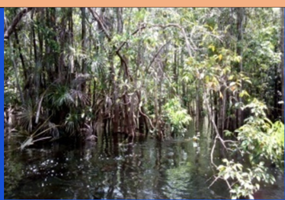 Water and Igapó (Wi)	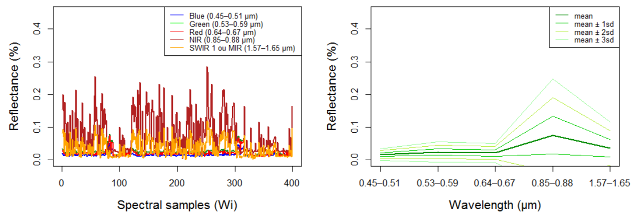
C7	 Sand (Sa)	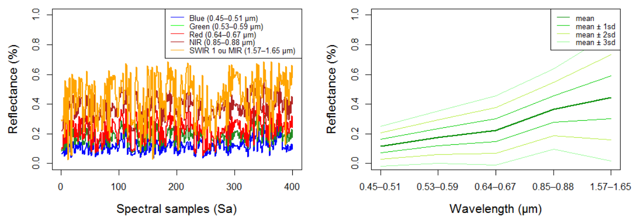
C8	 Urban area (Ua)	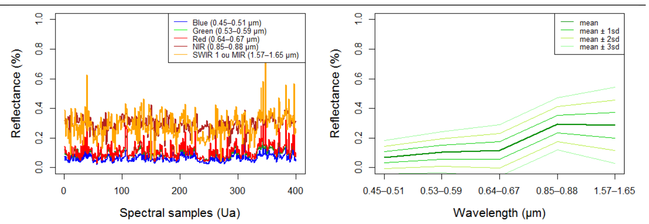

Table 2. *Cont.*

Class	Vegetation Cover and Land Use	Spectral Patterns	
C9	 Forest Degradation (Fd)	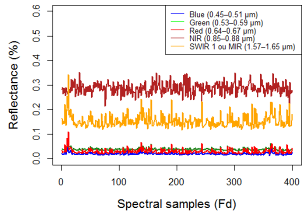	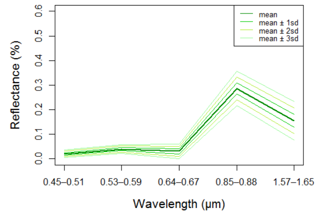
C10	 Pasture (Pa)	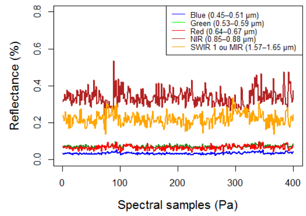	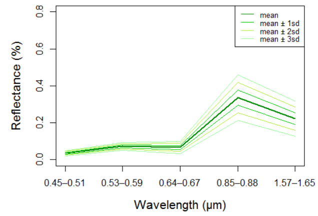
C11	 Deforestation (De)	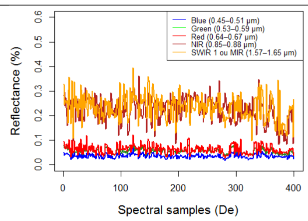	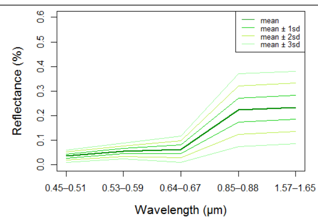

The spectral patterns of the 11 classes were considered statistically distinct in terms of their visible (RGB), near-infrared (NIR), and medium (SWIR 1 or MIR) bands (Table 3).

Table 3. Overall descriptive statistics of the reflectance values of ROI samples per pixel in terms of their visible (RGB) and infrared (NIR and SWIR 1 or MIR) bands.

Parameters/Bands	Blue	Green	Red	NIR	SWIR 1 or MIR
Landsat 8 (OLI)	**b2**	**b3**	**b4**	**b5**	**b6**
ROI samples	4400	4400	4400	4400	4400
Minimum	0.01	0.01	0.01	0.00	0.00
Maximum	0.41	0.50	0.57	0.65	0.86
Median	0.03	0.05	0.04	0.27	0.17
Average	0.04	0.06	0.06	0.26	0.19
$IC_{95\%\ Lower}$	0.04	0.06	0.06	0.26	0.19
$IC_{95\%\ Upper}$	0.04	0.06	0.07	0.26	0.20
Standard deviation	0.03	0.05	0.06	0.09	0.12
Variance	0.001	0.002	0.004	0.008	0.013
ANOVA	1122.9	1396.2	1547.0	1394.1	1327.0
p-value	0.000	0.000	0.000	0.000	0.000

Tukey's test for the comparison of means by pairs showed the formation of spectral groups with reflectance homogeneity in their electromagnetic spectrum bands (0.45–1.65 µm), with NIR presenting different spectral patterns in all classes (Table 4).

Table 4. Spectral group separation (SG) of the reflectance of ROI samples per pixel in their visible (RGB) and infrared (NIR and SWIR 1 or MIR) bands per vegetation cover and land-use class.

Blue (0.45–0.51 µm)				Green (0.53–0.59 µm)				Red (0.64–0.67 µm)				NIR (0.85–0.88 µm)				SWIR 1/MIR (1.57–1.65 µm)			
SG	Class	Mean	*p*	SG	Class	Mean	*p*	SG	Class	Mean	*p*	SG	Class	Mean	*p*	SG	Class	Mean	*p*
	C6	0.017		1	C6	0.025	1.0		C6	0.022		1	C6	0.076	1.0	1	C6	0.036	1.0
1	C1	0.017	1.0		C1	0.037		1	C1	0.022	1.0	2	C5	0.170	1.0		C1	0.134	
	C2	0.018		2	C2	0.040	1.0		C2	0.024		3	C4	0.212	1.0	2	C2	0.139	1.0
2	C9	0.021	1.0		C9	0.040		2	C9	0.031	1.0	4	C11	0.223	1.0		C3	0.140	
3	C3	0.024	1.0		C3	0.045			C3	0.034		5	C3	0.259	1.0	3	C9	0.154	1.0
4	C4	0.031	1.0	3	C5	0.047	1.0	3	C4	0.047	1.0	6	C9	0.286	1.0	4	C5	0.169	1.0
	C5	0.033			C4	0.049			C5	0.051		7	C8	0.294	1.0	5	C4	0.179	1.0
5	C10	0.035	1.0	4	C11	0.056	1.0	4	C11	0.064	1.0	8	C1	0.310	1.0	6	C10	0.222	1.0
	C11	0.036		5	C10	0.073	1.0		C10	0.067		9	C2	0.318	1.0	7	C11	0.234	1.0
6	C8	0.070	1.0	6	C8	0.104	1.0	5	C8	0.116	1.0	10	C10	0.337	1.0	8	C8	0.286	1.0
7	C7	0.117	1.0	7	C7	0.177	1.0	6	C7	0.224	1.0	11	C7	0.367	1.0	9	C7	0.446	1.0
MSE		0.0003		MSE		0.0005		MSE		0.0009		MSE		0.0020		MSE		0.0034	

Where: SG = spectral group; *p* = *p*-value; MSE = mean squared error; Tukey's test with pairwise means (α = 0.05).

The spectral correlations of the reflectance values of the ROI samples per pixel in the visible (RGB) and infrared (NIR and SWIR 1 or MIR) bands were addressed for the total variation (N = 4400) and per class (n = 400) (Figure 4).

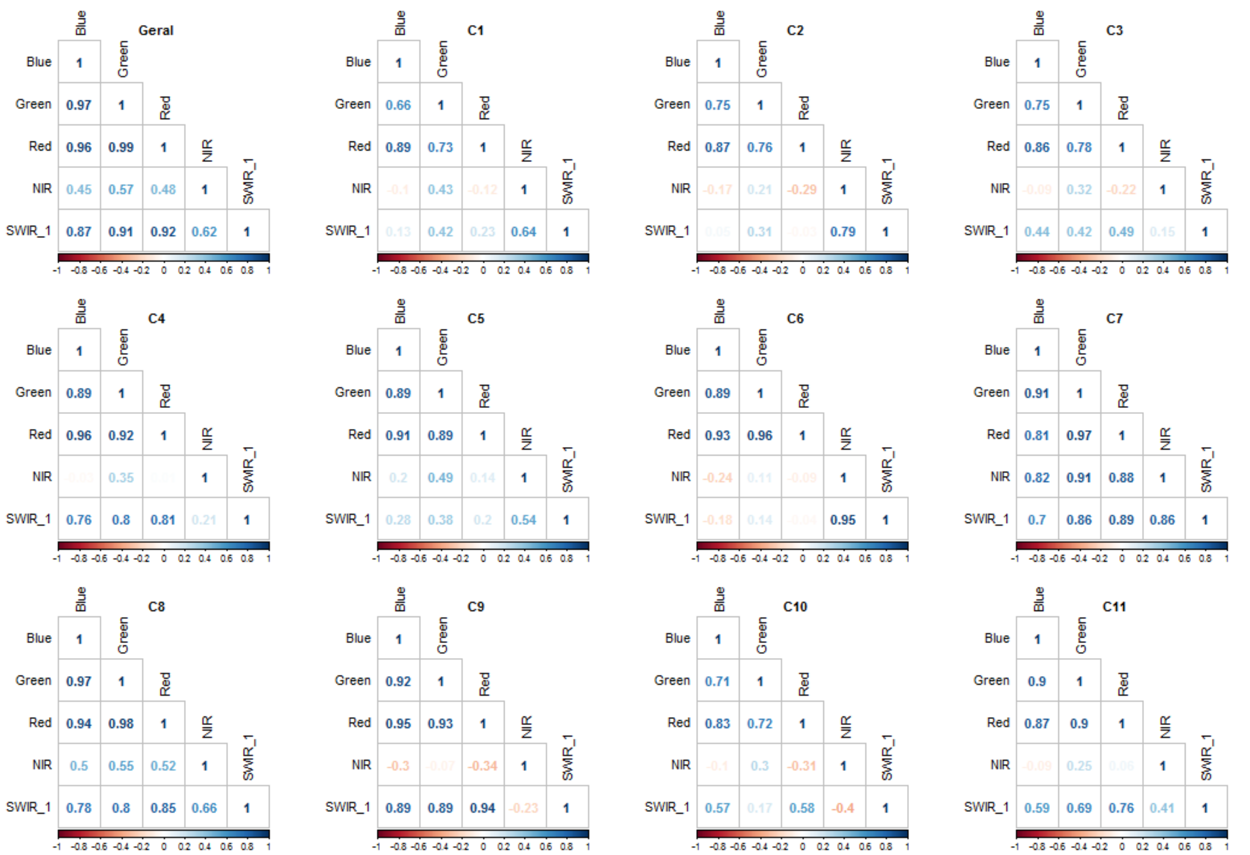

Figure 4. Spectral correlations among visible (RGB) and infrared (NIR and SWIR 1 or MIR) bands of general (N = 4400) and per class—C (n = 400) reflectance of ROI samples per pixel.

3.2. The Spectral and Spatial Behaviors of the Vegetation Indices and Fractional Coverage Images

The vegetation evidenced spectral reflectance behaviors with high indirect activities (remote sensing) of photosynthesis (NDVI, PV) and the presence of water in the internal structures of the plants (NDWI) in decreasing order in forest vegetation: Class 1, Class 2, Class 3, Class 4, and Class 5 (Table 5). The spectral and spatial behaviors of the vegetation index, water index, and fraction cover image within the Anauá National Forest can be visualized in Figure 5.

Table 5. Descriptive statistics of the spectral reflectance behaviors of NDVI, NDWI, and FCI in relation to the 11 vegetation cover and land-use classes of ROI samples per pixel (N = 4400).

Class	NDVI	NDWI	Fractional Coverage Image (FCI)		
			BARE (%)	PV (%)	NPV (%)
C1	0.86 ± 0.01	0.40 ± 0.02	0.97 ± 2.31	93.93 ± 2.06	8.64 ± 3.75
C2	0.86 ± 0.02	0.39 ± 0.02	2.09 ± 3.39	92.28 ± 2.85	8.14 ± 4.03
C3	0.77 ± 0.03	0.30 ± 0.06	0.25 ± 1.26	85.37 ± 6.62	19.33 ± 6.22
C4	0.64 ± 0.06	0.09 ± 0.09	0.04 ± 0.54	65.17 ± 13.00	46.74 ± 15.07
C5	0.53 ± 0.08	0.03 ± 0.16	0.06 ± 0.58	61.42 ± 23.44	43.10 ± 22.75
C6	0.43 ± 0.31	0.36 ± 0.11	0.12 ± 0.67	22.80 ± 40.12	2.87 ± 5.82
C7	0.25 ± 0.11	−0.08 ± 0.11	15.43 ± 23.07	13.41 ± 23.70	29.68 ± 34.16
C8	0.45 ± 0.16	0.03 ± 0.12	16.07 ± 18.64	35.47 ± 23.73	48.22 ± 21.91
C9	0.81 ± 0.06	0.30 ± 0.09	0.84 ± 2.20	85.25 ± 9.95	19.17 ± 11.07
C10	0.67 ± 0.06	0.20 ± 0.10	11.00 ± 10.15	64.97 ± 11.71	24.95 ± 15.99
C11	0.55 ± 0.13	−0.0267 ± 0.12	1.01 ± 3.46	50.64 ± 16.53	54.93 ± 20.81

Where values refer to the mean and standard deviation.

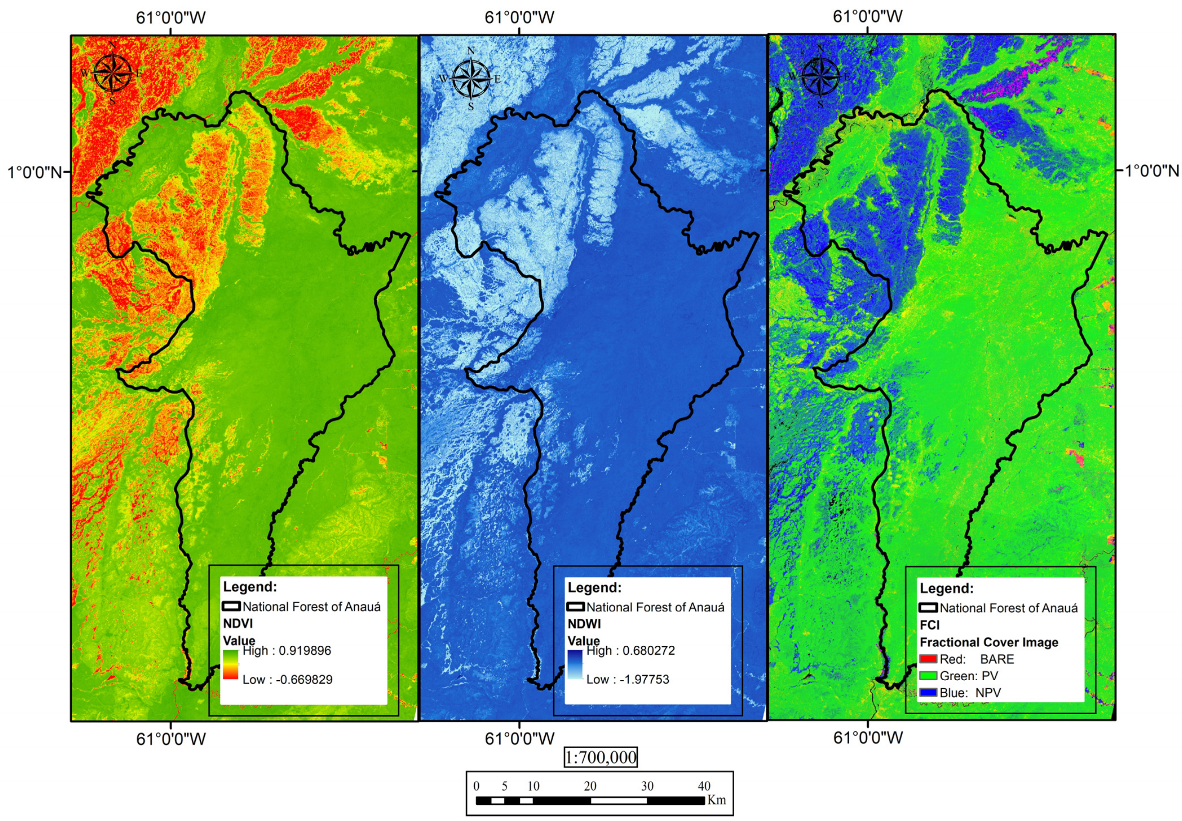

Figure 5. Spectral and Spatial reflectance behaviors of vegetation (NDVI), water (NDWI), and fractional cover image (PV, NPV, and BARE) indices of the Anauá National Forest in Roraima, Brazil.

3.3. Accuracy Assessment

Pixel-supervised classifications via the maximum likelihood algorithm demonstrated substantial accuracy in the 3 color compositions: visible [R(4)G(3)B(2), overall = 74.9%, Kappa = 0.72]; near infrared—NIR [R(5)G(4)B(3), overall = 76.9%, Kappa = 0.75]; and medium infrared—SWIR 1 or MIR [R(6)G(5)B(4), overall = 72.9%, Kappa = 0.70], see Supplementary Material. GEOBIA also demonstrated substantial accuracy [overall = 74.2%; Kappa = 0.72] for gathering spectral information from 5 bands of visible (RGB) and infrared (NIR and SWIR 1 or MIR) wavelengths, together with two vegetation indices (NDVI and NDWI), associated with a set of rules (descriptors) by class (Figure 3). The area of the Anauá National Forest in Roraima was delimited in the following classes by supervised pixel and GEOBIA classifications (Table 6).

Table 6. Delimitations of the estimated areas of the 11 vegetation cover and land-use classes of the supervised classifications by per-pixel and GEOBIA.

Class	Maximum Likelihood (Per-Pixel)						GEOBIA		
	R(4)G(3)B(2) (Km^2)	(%)	R(5)G(4)B(3) (Km^2)	(%)	R(6)G(5)B(4) (Km^2)	(%)	Anauá National Forest (Km^2)	(%)	Mosaic (Km^2)
C1	755	29	712	27	980	27	992	38	26,508
C2	1132	44	1169	45	898	45	807	31	16,560
C3	170	7	207	8	214	8	274	11	9096
C4	257	10	313	12	285	12	231	9	4395
C5	141	5	109	4	88	4	201	8	3451
C6	6	0	9	0	14	0	11	0	37,328
C7	2	0	2	0	3	0	26	1	1283
C8	10	0	5	0	3	0	8	0	501
C9	76	3	22	1	33	1	34	1	2439
C10	1	0	3	0	3	0	0	0	614
C11	45	2	45	2	75	2	0	0	30
Total	2596	100	2596	100	2596	100	2584	100	102,204

4. Discussion

The spectral behavior of radiation reflected, transmitted, or absorbed by vegetation has been investigated in attempts to understand the responses of natural systems to stress situations, forest degradation, disease, drought, fire, seasonality, floods, successional stages, etc., [8,17,25,26,45,46]. The spectroscopic canopy fingerprints of each species are strongly influenced by foliar chemical attributes (trace elements), specific leaf area (SLA), water content, lignin, cellulose, carbon, and the enzymatic activity of chlorophylls and carotene pigments and can generally be described by hyperspectral sensors and LIDAR (light detection and ranging) [46–51]. In this study, we observed that the spectral behavior of reflectance in the near-infrared (NIR) band (0.85–0.88 µm), obtained by the Landsat 8 sensors (OLI), revealed differential patterns, with the formation of spectral groups corresponding to 11 vegetation cover and land-use classes, making it possible to distinguish between forest phytophysiognomies in the northern Brazilian Amazon, particularly in the Anauá National Forest in Roraima State.

Reflectance analysis of three color compositions was used to visually explore the color and tone nuances of the electromagnetic spectrum between the visible (RGB) and infrared (NIR and SWIR 1 or MIR) bands characteristic of each vegetation cover and land-use class. The R(4)G(3)B(2) composition of the visible bands allows the visualization of the digital image in much the same way as we actually see it in nature, allowing a rapid distinction between natural, intact landscape elements (land cover including water = C1 to C7) and those altered by humans (land use = C8 to C11), with lower reflectance values for vegetation and water (C1 to C6) and higher values for land-use areas (C7 to C11) [2,22]. The R(5)G(4)B(3) composition of the near-infrared band (NIR) shows nuances in varied shades of red, referring to variations in texture (smooth to rough), with lighter tones being related to increased soil exposure, the chaotic mirroring behavior of the sand fraction, and high water absorption, thus demonstrating the great potential of NIR to distinguish between vegetation cover and land-use classes [22,24–26]. The R(6)G(5)B(4) composition of the medium infrared range (SWIR 1 or MIR) shows nuances between dry and flooded environments, with the vegetation absorbing more radiation in this range when it has higher water contents in leaf structures [22]. In natural environments, without stress (C1 to C5), medium infrared (SWIR 1 or MIR) absorption is greater than that observed in altered environments such as degraded forests (C9), pastures (C10), and deforested sites (C11). The spectral behaviors of the vegetation (NDVI) and water (NDWI) indices reflect these nuances among visible (red) and near and medium infrared (NIR and SWIR 1 or MIR) wavelengths, where the sources of variation between classes are related to differences in plant height and density and different degrees of soil exposure.

The maps of spectral reflectance patterns characteristic of vegetation cover and land-use classes can be termed spectral signatures and are of vital importance in supervised classifications by pixels or GEOBIA. Although the maximum likelihood algorithm per pixel is considered robust and rapidly processed, we have already reported problems associated with this purely statistical method [11–13]. In the present study, we detected errors associated with the Sand (C7), Campinara Gramíneo-Lenhosa (C5), and Urban Area (C8) classes. The GEOBIA approach presents numerous manners to create classification rules to reduce confusion among geographic objects in the landscape and obtain more satisfactory and realistic results [9–11]. The segmentation calibration process in GEOBIA is considered essential to obtaining satisfactory results, with subsequent segmentations designed to group geographic objects with specific levels of spectral similarity. We observed that the calibration of shape parameters (0.8) and compaction (0.7) resulted in geographic objects with well-delimited and less compact edges, although internal details related to color and tonality aspects, and considered essential for distinguishing among forest physiognomies (C1 to C5), were lost. Therefore, by reducing the shape (0.1) and compression (0.5) values, we can highlight the color and tonality of the geographic objects, giving greater weight to the near-infrared band (NIR), which is responsible for the largest variations among classes. The work in [9–11] reported that when assigning attributes to geographic objects, the spectral properties of the individual cells or pixels are calculated for the whole object, reducing the confusion of the classification as an average, and thus reducing variance (within the object). The association of NIR reflectance values with NDVI and NDWI in each set of rules per class can also be considered a spectral signature within the GEOBIA approach. Although a supervised classification per pixel achieved greater accuracy than GEOBIA in separating the spectral patterns of the 11 classes mapped in this study, we emphasize that the GEOBIA approach could be improved with further studies, especially in the context of tropical forests using NIR. The GEOBIA approach allows wide possibilities for calibration and the definition of a variable set of spectral rules associated with vegetation indices, spatial parameters, and associated statistics. Figure 6 presents the results of the pixel-supervised classification (in different compositions) and the GEOBIA classification of the spatial patterns of the forest phytophysiognomies mapped within the Anauá National Forest in Roraima, Brazil.

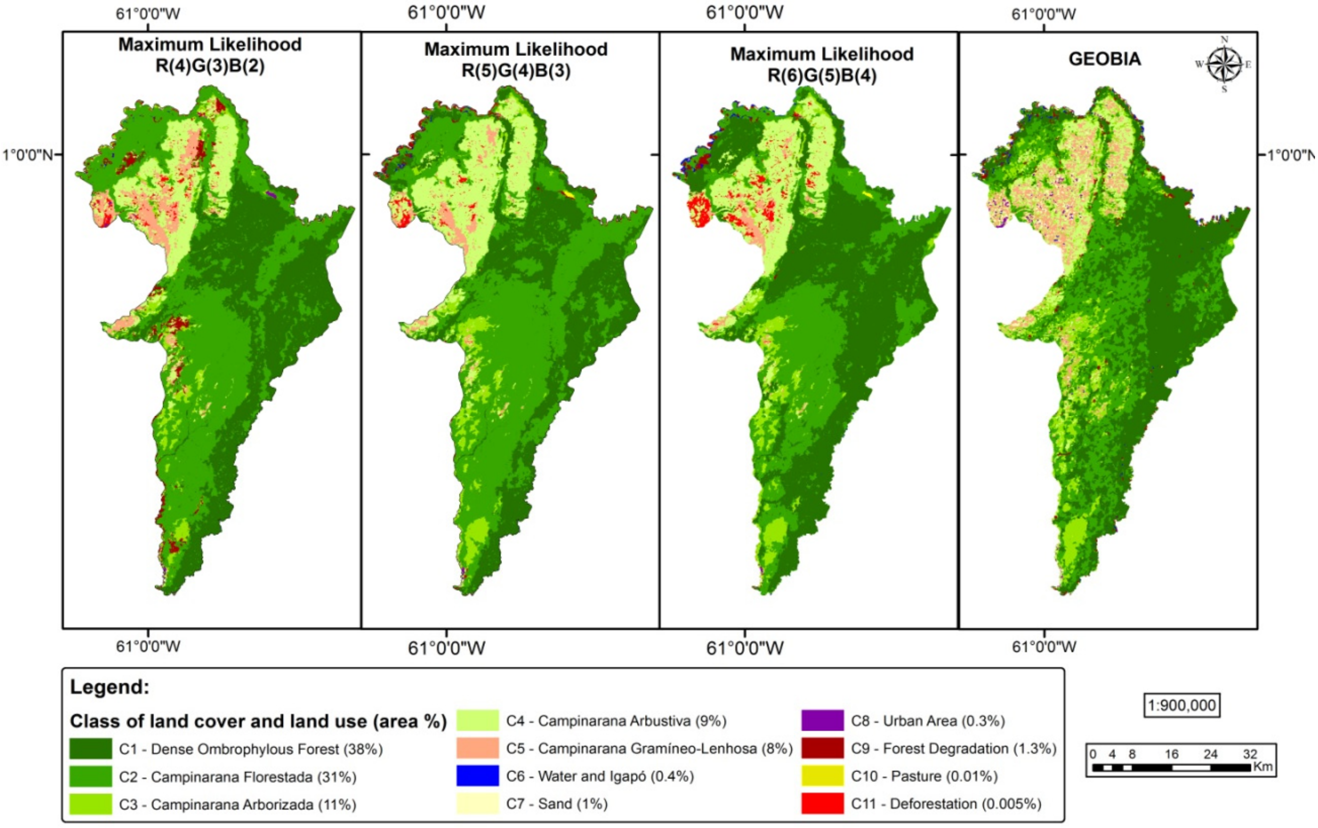

Figure 6. Pixel supervised classification in 3 color compositions (maximum likelihood) versus GEOBIA of the vegetation cover and land-use classes in the Anauá National Forest, Roraima State, Brazil, where area % expresses the percentage area per class as classified by GEOBIA.

The Anauá National Forest has great potential for sustainable forest management, considering that forest cover occupies the largest portion of land within this federal conservation area, even without considering permanent preservation areas (APP), which are legal instruments defining areas that must be preserved in riparian forests, bodies of water, etc., (Law 12.651 of 2012 of the New Forest Code of Brazil). However, the delay in preparing a management plan for the National Forest [36] made it impossible to carry out sustainable forest management activities for many years, leaving it vulnerable to deforestation, illegal selective logging, and forest fires [18]. It therefore failed to contribute to the socioeconomic development of southern Roraima, in the Brazilian Amazon.

GEOBIA estimated forest degradation by illegal selective logging within the Anauá National Forest to be 34 km^2 in the period between 2015 and 2017. Using the per-pixel method, this area varied between 22 and 76 km^2, considering different spectral band compositions (Table 6). The work in [44] developed 14 metrics to evaluate the textural features of satellite images based on co-occurrence matrix operations that statistically expressed spatial variations of gray tones and visually differentiated regions with smooth to rough textures. The Haralick texture contrast (GLMC Contrast all dir.) associated with a set of rules to understand the variation in the spatial distributions of gray tones [referring to reflectance values of visible (RGB) and infrared (NIR and SWIR 1 or MIR) bands] was used with substantial accuracy. The rule (Figure 3) that associates Descriptor 1 {NIR classified by reflectance (%) at the threshold of 0.2 (blue) to 0.4 (green)} with Descriptor 2 {Haralick texture contrast (GLCM Contrast all dir.)} allows the spectral separation of Dense Ombrophilous Forest (C1) from Campinarana Florestada (C2) and is considered a spectral signature within the GEOBIA approach (Figure 7).

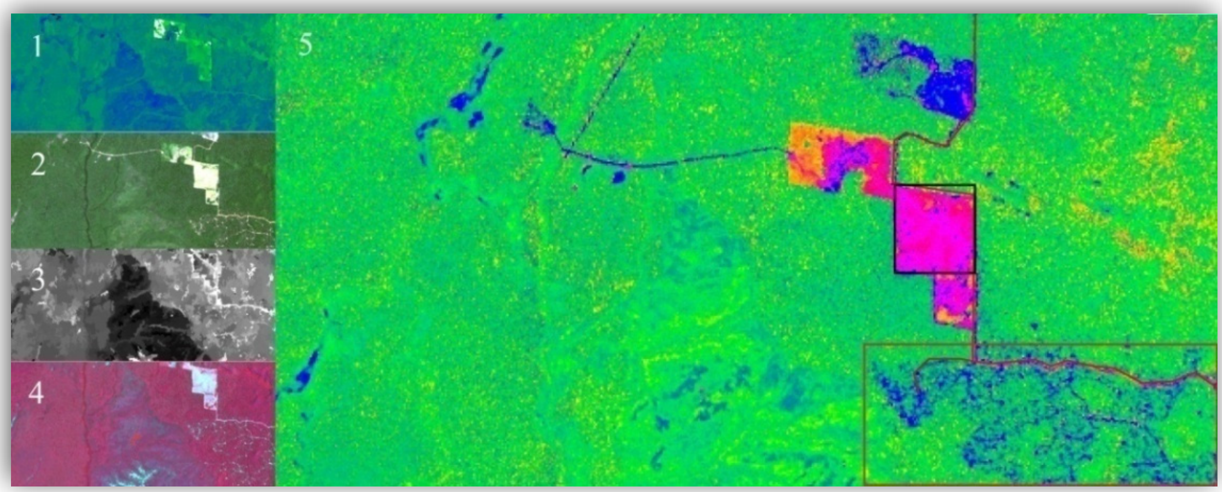

Figure 7. Spectral and spatial patterns of vegetation cover and land-use classes in the Anauá National Forest, in which: (**1**) Descriptor 1 {NIR classified by reflectance (%) at the threshold of 0.2 (blue) to 0.4 (green)}; (**2**) green vegetation in the visible range (RGB); (**3**) Descriptor 2 {Haralick texture contrast (GLCM Contrast all dir.)} showing light tones in areas of high contrast (rough texture) and dark tones in areas of lower contrast (smooth texture); (**4**) red vegetation in the near-infrared range—NIR; and, (**5**) fractional cover imaging, evidencing the high percentages of exposed soil (Bare in pink) resulting from deforestation (black square), and high concentrations of dead vegetation (NPV in blue), and forest degradation (red rectangle) resulting from selective timber extraction.

Deforestation (C11, black square) and forest degradation (C9, red rectangle) are land-use classes with different spatial patterns (Figure 7). Deforestation is easily detected by medium (e.g., Landsat 8, 30 m) and high spatial resolution (e.g., QuickBird, 0.6 cm to 2.8 m) satellite images and is usually associated with more compact, man-made outlines related to pasture formation, cattle ranching, and agricultural crops after forest clearing and burning [33,34]. Forest degradation has been almost invisible to most satellite coverage [16] because it represents man-made attempts to hide illegal extraction by maintaining the canopy cover which cannot be identified by medium to low resolution satellite coverage (Landsat sensors: 15–120 m to NOAA: 1.1 Km) [14,15]. In this way, both land uses cause reductions in native forest tree species diversity and contribute to the loss of environmental services in the Amazon [19,35,52,53].

Both land-use classes in southern Roraima, near the Anauá National Forest, are strongly related to the formation of pasturelands through deforestation and illegal selective logging [17]. These actions can be captured by changes in the proportions of the PV, NPV, and Bare fractions in coverage images, and changes in spectral values (bands: blue, green, red, NIR, and SWIR or MIR), with reductions of NDVI and NDWI values that reflect reductions of photosynthetic capacity and water accumulation by the vegetation. We can therefore observe how changes in land use and land cover determine reductions of biomass and forest carbon stocks—resulting in significant changes in the spectral behavior of vegetation cover reflectance in the Amazon (Figure 8). We emphasize that the spectral patterns of vegetation cover may also change over the years due to the occurrence of both natural environmental factors (drought, mortality, fire, storms, etc.) and anthropogenic factors (mainly those related to land-use expansion) [45–51].

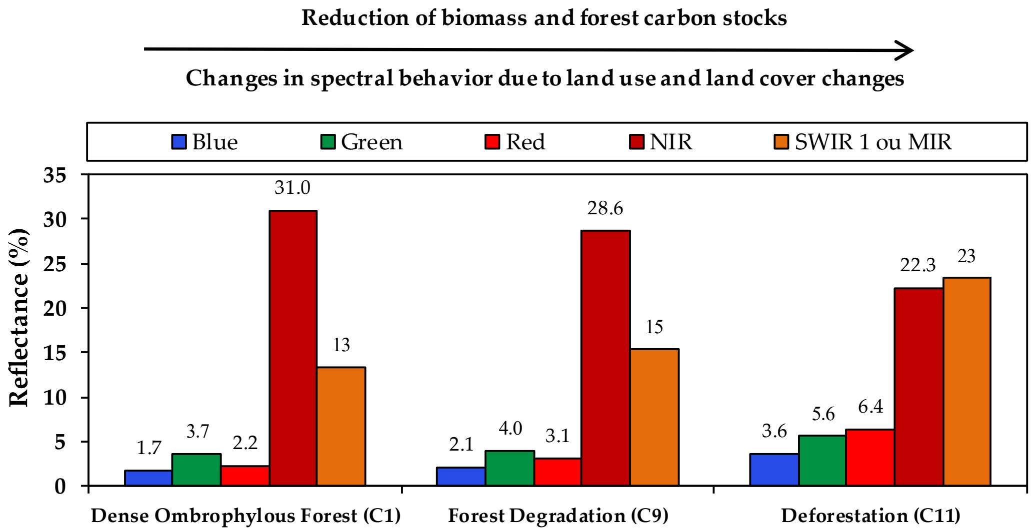

Figure 8. Changes in land use and land cover provoke reductions of biomass and carbon stocks, with changes in the spectral behavior of vegetation reflectance in the Amazon. Images from Landsat 8 (OLI).

Many conservation areas in Brazil were created to contain the advance of illegal and predatory extraction of natural resources from natural lands and jurisdictional waters and to promote the maintenance of biological diversity and protect genetic resources (ICMBio Law 9985). The Anauá National Forest is a sustainable use area whose basic objective is to guarantee the multiple sustainable uses of forest resources in association with scientific research. The maps created here (Figures 5–7) were donated to ICMBio [36], the managing body of the Anauá National Forest, to subsidize technical-scientific discussions of the delimitation, management, and monitoring of the permanent preservation areas, guarantee the maintenance of the vital processes of the fauna and flora, and protect legal reserves for the sustainable and rational extraction of forest resources. We believe that sustainable forest management is the best way to preserve forest integrity, the economic viability of forest activities, the conservation of the environmental services provided by the Amazon Forest, and to help maintain Earth's climatic balance.

5. Conclusions

The mapping of vegetation cover and land use via Landsat 8 (OLI) sensors in the visible and infrared bands (0.45–1.65 µm) enabled the separation and distinction of spectral patterns of different forest phytophysiognomies—a strategic achievement for the management of natural resources within conservation areas in the Amazon region.

We conclude that both supervised classification methods (pixel-based—maximum likelihood; and geographic object-based image analysis—GEOBIA) were accurate for distinguishing the spectral patterns of the different phytophysiognomies in the Anauá National Forest in Roraima State, Brazil. We emphasize, however, that the GEOBIA approach requires further study, considering that it allows wide possibilities for the calibration and definition of variable sets of spectral rules associated with vegetation indices, spatial parameters, and associated statistics.

The Anauá National Forest has great potential for sustainable forest management, considering its large area, with the predominance of Dense Ombrophilous Forests (C1) and Campinarana Florestada (C2). A lack of effective management, however, puts its flora and environmental services at risk due to increasing carbon emissions to the atmosphere from human activities associated with deforestation for expansion of cattle ranching, forest degradation through illegal selective logging, and forest fires.

Supplementary Materials: The following supporting information can be downloaded at: https://www.mdpi.com/article/10.3390/ecologies4040045/s1, Figure S1: Confusion matrix (or error matrix) for the maximum likelihood classification (per-pixel). Where: Color composition R(4)G(3)B(2); mosaic of reflectance images (path 232; rows 059-060); Landsat 8 sensor (OLI). Figure S2: Confusion matrix (or error matrix) for the maximum likelihood classification (per-pixel). Where: Color composition R(5)G(4)B(3); mosaic of reflectance images (path 232; rows 059-060); Landsat 8 sensor (OLI). Figure S3: Confusion matrix (or error matrix) for the maximum likelihood classification (per-pixel). Where: Color composition R(6)G(5)B(4); mosaic of reflectance images (path 232; rows 059-060); Landsat 8 sensor (OLI). Figure S4: Confusion matrix (or error matrix) for the GEOBIA. Where: using visible bands (RGB), near and medium infrared bands (NIR, SWIR 1 or MIR), NDVI and NDWI; mosaic of reflectance images (path 232; rows 059-060); Landsat 8 sensor (OLI).

Author Contributions: All authors participated equally in the experimental design, data analysis, and manuscript preparation. All authors have read and agreed to the submitted version of the manuscript.

Funding: Coordenação de Aperfeiçoamento de Pessoal de Nível Superior (CAPES): 1451925.

Institutional Review Board Statement: Not applicable.

Informed Consent Statement: Not applicable.

Data Availability Statement: The datasets generated and/or analyzed during this exploratory study are available from the corresponding author. Data will be shared upon reasonable request.

Acknowledgments: We thank the professionals of the National Institute of Amazonian Research (INPA), the scientific support of the team of Philip Fearnside, the professionals who participated in the river expedition to southern Roraima (the "Sirenians") financed by the ICMBio of Roraima, as well as the students and professionals of the State University of Roraima (UERR) who supported our efforts.

Conflicts of Interest: The authors declare no conflict of interest.

References

1. Bolstad, P.V.; Lillesand, T.M. Rapid Maximum Likelihood Classification. *Phot. Eng. Rem. Sens.* **1991**, *57*, 67–74.
2. Richards, J.A.; Jia, X. *Rem. Sens. Digital Image Analysis—An Introduction*, 4th ed.; Springer: Berlin/Heidelberg, Germany, 2006.
3. Benz, U.C.; Hofmann, P.; Willhauck, G.; Lingenfelder, I.; Heynen, M. Multi-resolution, object-oriented fuzzy analysis of remote sensing data for GIS-ready information. *ISPRS J. Phot. Rem. Sens.* **2004**, *58*, 239–258. [CrossRef]
4. Walter, V. Object-based classification of remote sensing data for change detection. *ISPRS J. Phot. Rem. Sens.* **2004**, *58*, 225–238. [CrossRef]
5. Chubey, M.S.; Franklin, S.E.; Wulder, M.A. Object-based Analysis of Ikonos-2 Imagery for Extraction of Forest Inventory Parameters. *Phot. Eng. Rem. Sens.* **2006**, *72*, 383–394. [CrossRef]
6. Bontemps, S.; Bogaert, P.; Titeux, N.; Defourny, P. An object-based change detection method accounting for temporal dependences in time series with medium to coarse spatial resolution. *Remote Sens. Environ.* **2008**, *112*, 3181–3191. [CrossRef]
7. Blaschke, T. Object based image analysis for remote sensing. *ISPRS J. Photo. Remote Sens.* **2010**, *65*, 2–16. [CrossRef]
8. Lyons, M.B.; Roelfsema, C.M.; Phinn, S.R. Towards understanding temporal and spatial dynamics of seagrass landscapes using time-series remote sensing. *Est., Coast. Shelf Sci.* **2013**, *120*, 42–53. [CrossRef]
9. Hay, G.J.; Castilla, G. Geographic Object-Based Image Analysis (GEOBIA): A new name for a new discipline. In *Object-Based Image Analysis, Lecture Notes in Geoinformation and Cartography*; Blaschke, T., Lang, S., Hay, G.J., Eds.; Springer: Berlin/Heidelberg, Germany, 2008; pp. 75–89. [CrossRef]
10. Blaschke, T.; Hay, G.J.; Kelly, M.; Lang, S.; Hofmann, P.; Addink, E.; Feitosa, R.Q.; van der Meer, F.; van der Werff, H.; van Coillie, F.; et al. Geographic Object-Based Image Analysis—Towards a new paradigm. *ISPRS J. Photo. Remote Sens.* **2014**, *87*, 180–191. [CrossRef]
11. Watmough, G.R.; Palm, C.A.; Sullivan, C. An operational framework for object-based land use classification of heterogeneous rural landscapes. *Int. J. Appl. Earth Observ. Geoinform.* **2017**, *54*, 134–144. [CrossRef]
12. Fisher, P. The pixel: A snare and a delusion. *Inter. J. Remote Sens.* **1997**, *18*, 679–685. [CrossRef]
13. Blaschke, T.; Strobl, J. What's Wrong with Pixels? Some Recent Developments Interfacing Remote Sensing and GIS. *Z. Fur Geoinf. Syst.* **2001**, *14*, 12–17.
14. Kelly, M.; Blanchard, S.D.; Kersten, E.; Koy, K. Terrestrial Remotely Sensed Imagery in Support of Public Health: New Avenues of Research Using Object-Based Image Analysis. *Rem. Sens.* **2011**, *3*, 2321–2345. [CrossRef]
15. Pereira, R., Jr.; Zweede, J.; Asner, G.P.; Keller, M. Forest canopy damage and recovery in reduced-impact and conventional selective logging in eastern Para, Brazil. *For. Ecol. Manag.* **2002**, *168*, 77–89. [CrossRef]

16. Asner, G.P.; Knapp, D.E.; Broadbent, E.N.; Oliveira, P.J.C.; Keller, M.; Silva, J.N.M. Selective Logging in the Brazilian Amazon. *Science* **2005**, *310*, 480–482. [CrossRef] [PubMed]
17. Asner, G.P.; Knapp, D.E.; Balaji, A.; Paez-Acosta, G. Automated mapping of tropical deforestation and forest degradation: CLASlite. *J. Appl. Remote Sens.* **2009**, *3*, 033543. [CrossRef]
18. Condé, T.M.; Higuchi, N.; Lima, A.J.N. Illegal selective logging and forest fires in the Northern Brazilian Amazon. *Forests* **2019**, *10*, 61. [CrossRef]
19. Higuchi, N.; Santos, J.; Ribeiro, R.J.; Minette, L.; Biot, Y. Biomassa da Parte Aérea da Vegetação da Floresta Tropical Úmida de Terra-firme da Amazônia Brasileira. *Acta Amazon.* **1998**, *28*, 153–166. [CrossRef]
20. Fearnside, P.M.; Barbosa, R.I.; Pereira, V.B. Emissões de gases do efeito estufa por desmatamento e incêndios florestais em Roraima: Fontes e sumidouros. *Agro@Mbiente* **2013**, *7*, 95–111. [CrossRef]
21. Ichoku, C.; Karnieli, A. A review of mixture modeling techniques for sub-pixel land cover estimation. *Rem. Sens. Rev.* **1996**, *13*, 161–186. [CrossRef]
22. Jensen, J.R. *Sensoriamento Remoto do Ambiente: Uma Perspectiva em Recursos Terrestres*, 2nd ed.; Prentice Hall Series in Geographic Information Science/Parêntesis: São Paulo, Brazil, 2009.
23. James, G.; Witten, D.; Hastie, T.; Tibshirani, R. *An Introduction to Statistical Learning with Applications in R*, 1st ed.; Springer: New York, NY, USA, 2013.
24. Durgante, F.M.; Higuchi, N.; Almeida, A.; Vicentini, A. Species Spectral Signature: Discriminating closely related plant species in the Amazon with Near-Infrared Leaf-Spectroscopy. *For. Ecol. Manag.* **2013**, *291*, 240–248. [CrossRef]
25. Carter, G.A.; Knapp, A.K. Leaf optical properties in higher plants: Linking spectral characteristics to stress and chlorophyll concentration. *Am. J. Bot.* **2001**, *88*, 677–684. [CrossRef] [PubMed]
26. Ponzoni, F.J.; Resende, A.C.P. Caracterização espectral de estágios sucessionais de vegetação secundária arbórea em Altamira (PA), através de dados orbitais. *R. Árvore* **2004**, *28*, 535–545. [CrossRef]
27. Hopkins, M.J.G. Modelling the known and unknown plant biodiversity of the Amazon Basin. *J. Biogeog.* **2007**, *34*, 1400–1411. [CrossRef]
28. Condé, T.M.; Tonini, H. Fitossociologia de uma Floresta Ombrófila Densa na Amazônia Setentrional, Roraima, Brasil. *Acta Amaz.* **2013**, *43*, 247–260. [CrossRef]
29. Adeney, J.M.; Christensen, N.L.; Vicentini, A.; Cohn-Haft, M. White-sand Ecosystems in Amazonia. *Biotropica* **2016**, *48*, 7–23. [CrossRef]
30. Guevara, J.E.; Damasco, G.; Baraloto, C.; Fine, P.V.A.; Peñuela, M.C.; Castilho, V.C.; Vincentini, A.; Cárdenas, D.; Wittmann, F.; Targhetta, N.; et al. Low Phylogenetic Beta Diversity and Geographic Neo-endemism in Amazonian White-sand Forests. *Biotropica* **2016**, *48*, 34–46. [CrossRef]
31. Anderson, A.B. White-sand vegetation of Brazilian Amazonia. *Biotropica* **1981**, *13*, 199–210. [CrossRef]
32. Mendonça, B.A.F.; Filho, E.I.F.; Schaefer, C.E.G.R.; Simas, F.N.B.; Paula, M.D. The soils of "Campinaranas" in Brazilian Amazon: Oligothrophic Sandy Ecosystems. *Ciência Florest.* **2015**, *25*, 827–839. [CrossRef]
33. Asner, G.P.; Townsend, A.R.; Bustamante§, M.M.C.; Nardoto, G.B.; Olander, L.P. Pasture degradation in the central Amazon: Linking changes in carbon and nutrient cycling with remote sensing. *Glob. Change Biol.* **2004**, *10*, 844–862. [CrossRef]
34. Nepstad, D.; McGrath, D.; Stickler, C.; Alencar, A.; Azevedo, A.; Swette, B.; Bezerra, T.; DiGiano, M.; Shimada, J.; Motta, R.S.; et al. Slowing Amazon deforestation through public policy and interventions in beef and soy supply chains. *Science* **2014**, *344*, 1118–1124. [CrossRef]
35. Dionisio, L.F.S.; Condé, T.M.; Gomes, J.P.; Martins, W.B.R.; Silva, M.W.; Silva, M.T. Caracterização morfométrica de árvores solitárias de *Bertholletia excelsa* H.B.K. no sudeste de Roraima. *Rev. Agro@Mbiente Line* **2017**, *11*, 163–173. [CrossRef]
36. ICMBio. Chico Mendes Institute of Biodiversity. PAN Portaria n° 457. Plano de Manejo da Floresta Nacional de Anauá. 2022. Available online: https://www.gov.br/icmbio/pt-br/assuntos/biodiversidade/unidade-de-conservacao/unidades-de-biomas/amazonia/lista-de-ucs/flona-de-anaua/arquivos/pm_flona_anaua_consolidado_vs-10.pdf (accessed on 27 September 2023).
37. IBGE. Brazilian Institute of Geography and Statistics. Manual Técnico da Vegetação Brasileira. Available online: https://biblioteca.ibge.gov.br/index.php/biblioteca-catalogo?view=detalhes&id=263011 (accessed on 1 March 2023).
38. ICMBio. Chico Mendes Institute of Biodiversity. PAN Sirênios. Plano de Ação Nacional para a Conservação dos Sirênios Peixe-boi-da-Amazônia (Trichechus inunguis) e Peixe-Boi Marinho (Trichechus manatus manatus). 2011. Available online: https://www.gov.br/icmbio/pt-br/assuntos/biodiversidade/pan/pan-sirenios/1-ciclo/pan-sirenios-livro.pdf (accessed on 1 February 2023).
39. USGS. United States Geological Survey. Landsat Missions Timeline—Landsat 8. Available online: https://landsat.usgs.gov/landsat-8-history (accessed on 2 July 2017).
40. R Development Core Team. R: A Language and Environment for Statistical Computing. Available online: http://www.R-project.org (accessed on 1 July 2022).
41. Gao, B.C. NDWI—A normalized difference water index for remote sensing of vegetation liquid water from space. *Rem. Sens. Environ.* **1996**, *58*, 257–266. [CrossRef]
42. Jin, S.; Sader, S.A. MODIS time-series imagery for forest disturbance detection and quantification of patch size effects. *Remote Sens. Environ.* **2005**, *99*, 462–470. [CrossRef]

43. Landis, J.R.; Koch, G.G. The Measurement of Observer Agreement for Categorical Data. *Biometrics* **1977**, *33*, 159–174. [CrossRef] [PubMed]
44. Haralick, R.M.; Shanmugam, K.; Dinstein, I. Textural Features for Image Classification. *IEEE Trans. Syst. Man Cybernet.* **1973**, *6*, 610–621. [CrossRef]
45. Gates, D.M.; Keegan, H.J.; Schleter, J.C.; Weidner, V.R. Spectral properties of plants. *Appl. Opt.* **1965**, *4*, 11–20. [CrossRef]
46. Rock, B.N.; Vogelmann, J.E.; Williams, D.L.; Vogelmann, A.F.; Hoshizaki, T. Remote Detection of Forest Damage: Plant responses to stress may have spectral "signatures" that could be used to map, monitor, and measure forest damage. *BioScience* **1986**, *36*, 439–445. [CrossRef]
47. Kodani, E.; Awaya, Y.; Tanaka, K.; Matsumura, N. Seasonal patterns of canopy structure, biochemistry and spectral reflectance in a broad-leaved deciduous *Fagus crenata* canopy. *For. Ecol. Manag.* **2002**, *167*, 233–249. [CrossRef]
48. Asner, G.P.; Martin, R.E.; Knapp, D.E.; Tupayachi, R.; Anderson, C.; Carranza, L.; Martinez, P.; Houcheime, M.; Sinca, F.; Weiss, P. Spectroscopy of canopy chemicals in humid tropical forests. *Rem. Sens. Environ.* **2011**, *115*, 3587–3598. [CrossRef]
49. Blackburn, G.A. Hyperspectral remote sensing of plant pigments. *J. Exp. Bot.* **2007**, *58*, 855–867. [CrossRef]
50. Asner, G.P.; Martin, R.E. Airborne spectranomics: Mapping canopy chemical and taxonomic diversity in tropical forests. *Front. Ecol. Environ.* **2008**, *7*, 269–276. [CrossRef]
51. Asner, G.P.; Martin, R.E.; Carranza-Jiménez, L.; Sinca, F.; Tupayachi, R.; CMartinez, P. Functional and biological diversity of foliar spectra in tree canopies throughout the Andes to Amazon region. *New Phytol.* **2014**, *204*, 127–139. [CrossRef]
52. Davidson, E.A.; Araújo, A.C.; Artaxo, P.; Balch, J.K.; Brown, I.F.; Bustamante, M.M.C.; Coe, M.T.; DeFries, R.S.; Keller, M.; Longo, M.; et al. The Amazon basin in transition. *Nature* **2012**, *481*, 321–328. [CrossRef] [PubMed]
53. Condé, T.M.; Tonini, H.; Higuchi, N.; Higuchi, F.G.; Lima, A.J.N.; Barbosa, R.I.; Pereira, T.S.; Haas, M.A. Effects of sustainable forest management on tree diversity, timber volumes, and carbon stocks in an ecotone forest in the northern Brazilian Amazon. *Land Use Policy* **2022**, *119*, 106145. [CrossRef]